



TITLE:

Atomic displacement in the CrMnFeCoNi high-entropy alloy – A scaling factor to predict solid solution strengthening

AUTHOR(S):

Okamoto, Norihiko L.; Yuge, Koretaka; Tanaka, Katsushi; Inui, Haruyuki; George, Easo P.

CITATION:

Okamoto, Norihiko L. ...[et al]. Atomic displacement in the CrMnFeCoNi high-entropy alloy – A scaling factor to predict solid solution strengthening. AIP Advances 2016, 6(12): 125008.

ISSUE DATE:

2016-12-01

URL:

<http://hdl.handle.net/2433/218241>

RIGHT:

© 2016 Author(s). This article is distributed under a Creative Commons Attribution (CC BY) License.

Atomic displacement in the CrMnFeCoNi high-entropy alloy – A scaling factor to predict solid solution strengthening

Norihiko L. Okamoto, Koretaka Yuge, Katsushi Tanaka, Haruyuki Inui, and Easo P. George

Citation: [AIP Advances](#) **6**, 125008 (2016); doi: 10.1063/1.4971371

View online: <http://dx.doi.org/10.1063/1.4971371>

View Table of Contents: <http://aip.scitation.org/toc/adv/6/12>

Published by the [American Institute of Physics](#)

Articles you may be interested in

[Alloy design for intrinsically ductile refractory high-entropy alloys](#)

[AIP Advances](#) **120**, 164902164902 (2016); 10.1063/1.4966659

[Mechanisms of plastic deformation in \[1 \$\bar{1}\$ 1\]-oriented single crystals of FeNiMnCrCo high entropy alloy](#)

[AIP Advances](#) **1783**, 020090020090 (2016); 10.1063/1.4966383

[Preferred site occupation and magnetic properties of Ni-Fe-Ga-Co ferromagnetic shape memory alloys by first-principles calculations](#)

[AIP Advances](#) **6**, 125007125007 (2016); 10.1063/1.4971822

[Impact of aluminum doping on the thermo-physical properties of refractory medium-entropy alloys](#)

[AIP Advances](#) **121**, 015105015105 (2017); 10.1063/1.4973489

HAVE YOU HEARD?

Employers hiring scientists and
engineers trust

PHYSICS TODAY | JOBS

www.physicstoday.org/jobs





Atomic displacement in the CrMnFeCoNi high-entropy alloy – A scaling factor to predict solid solution strengthening

Norihiko L. Okamoto,^{1,2,a} Koretaka Yuge,¹ Katsushi Tanaka,³ Haruyuki Inui,^{1,2} and Easo P. George^{4,b}

¹*Department of Materials Science and Engineering, Kyoto University, Kyoto 606-8501, Japan*

²*Center for Elements Strategy Initiative for Structure Materials (ESISM), Kyoto University, Kyoto 606-8501, Japan*

³*Department of Mechanical Engineering, Kobe University, Nada-ku, Kobe 657-8501, Japan*

⁴*Materials Science and Technology Division, Oak Ridge National Laboratory, Oak Ridge, Tennessee 37831, USA*

(Received 30 September 2016; accepted 20 November 2016; published online 6 December 2016)

Although metals strengthened by alloying have been used for millennia, models to quantify solid solution strengthening (SSS) were first proposed scarcely seventy years ago. Early models could predict the strengths of only simple alloys such as dilute binaries and not those of compositionally complex alloys because of the difficulty of calculating dislocation-solute interaction energies. Recently, models and theories of SSS have been proposed to tackle complex high-entropy alloys (HEAs). Here we show that the strength at 0 K of a prototypical HEA, CrMnFeCoNi, can be scaled and predicted using the root-mean-square atomic displacement, which can be deduced from X-ray diffraction and first-principles calculations as the isotropic atomic displacement parameter, that is, the average displacements of the constituent atoms from regular lattice positions. We show that our approach can be applied successfully to rationalize SSS in FeCoNi, MnFeCoNi, MnCoNi, MnFeNi, CrCoNi, CrFeCoNi, and CrMnCoNi, which are all medium-entropy subsets of the CrMnFeCoNi HEA. © 2016 Author(s). All article content, except where otherwise noted, is licensed under a Creative Commons Attribution (CC BY) license (<http://creativecommons.org/licenses/by/4.0/>). [<http://dx.doi.org/10.1063/1.4971371>]

Pure metals, for example, gold and silver, tend to be very soft; consequently, alloys such as 18-carat gold and sterling silver are used instead. In structural applications, where strength is an important requirement, pure metals are almost never used and alloys of various kinds are the norm. That alloying elements can strengthen metals has been known for thousands of years dating back to at least the Bronze Age. But the underlying mechanisms were identified relatively recently. For example, one of the ways in which alloying elements strengthen metals is by solid solution strengthening (SSS): solute atoms dissolved in a solvent matrix offer resistance to the motion of dislocations thereby making the material stronger. The first models that attempted to quantify this effect were introduced about seven decades ago;^{1–4} since then, many refinements have been proposed, continuing to the present.^{5–15}

Recently, complex solid solutions comprising multiple principal elements, often referred to as high-entropy alloys (HEAs), a name coined by Yeh et al. [Ref. 16], have been receiving tremendous attention in the literature [e.g., Refs. 17–22]. At least part of this interest stems from the fact that some of them exhibit intriguing and exceptional mechanical properties that are challenging to interpret. For example, the equiatomic HEA in the Cr-Mn-Fe-Co-Ni system with the face-centered cubic (FCC) structure,²³ exhibits peculiar mechanical properties, such as significant

^aCorresponding author, email: okamoto.norihiko.7z@kyoto-u.ac.jp

^bPresent address: Institute for Materials, Ruhr University Bochum, Universitätsstr. 150, Bochum 44801, Germany.



temperature dependence of yield strength^{24,25} with moderate strain-rate sensitivity,²⁴ and positive correlation between strength and ductility/toughness at cryogenic temperatures,¹⁷ which cannot be easily explained as the behavior of a simple FCC solid solution. Nevertheless, some sort of SSS must lie at the heart of the observed strength and it is important to develop a better understanding of its mechanism.

SSS mechanisms are generally described in terms of randomly dispersed substitutional solute atoms interacting with dislocations through misfits in the atomic size and elastic modulus of solute and solvent atoms. Models that treat stationary solute atoms acting on moving dislocations are of the frictional type and are divided roughly into two groups, depending on solute spacing, range of interaction, and solute-dislocation interaction energy (force).^{26,27} In very dilute alloys (concentrations of ~ 0.1 at.%), solute atoms adjacent to glide planes are assumed to come into contact with dislocations at full interaction force (this corresponds to the strong pinning, Fleischer-Friedel situation³). In concentrated alloys (several at.% of solute), a range of interaction forces is assumed (with the maximum value being of the same order as the above full interaction force) to account for spatial fluctuations of solute (obstacle) density (this corresponds to the weak pinning, Mott-Labusch situation⁴). The key parameter in models of SSS is the solute-dislocation interaction energy (force). Although this parameter can be calculated analytically using elasticity theory of dislocations, it can also be determined from first principles so that both elastic and chemical contributions are included. Indeed, Curtin and his co-workers⁵⁻⁷ have recently succeeded in explaining the solute concentration and temperature dependences of the critical resolved shear stress of certain dilute Al and Mg alloys by using an analytical model of the weak-pinning type in which the solute-dislocation interaction energy calculated from first principles was used as input. However, this approach cannot readily be applied to HEAs, because of the difficulties in calculating the solute-dislocation interaction energy. For example in an equiatomic HEA, “solute” and “solvent” atoms cannot be clearly defined. In a quinary HEA such as CrMnFeCoNi, the concentration of the constituent atoms is as high as 20 at.%. Clearly, alternative approaches to SSS are needed to describe the strength of HEAs.

Recently, Toda-Caraballo *et al.*^{9,10,13} have proposed an extension of a classical SSS model for binary systems⁴ to multicomponent systems, where the key parameters are the alloy’s calculated unit cell parameter and its variation with composition. Curtin and co-workers⁸ put forward a parameter-free and predictive SSS theory by approximating the multicomponent matrix as an effective medium having the average properties of the alloy and then calculated the solute-dislocation interaction energy from first principles for a multitude of configurations.

An alternative approach to those discussed above is to consider the displacement of the atoms in a solid solution from their ideal lattice positions. Solute-dislocation interaction energy (force) calculations usually assume that the solvent atoms around a solute atom are displaced from the ideal lattice positions due to a spherically symmetric strain field arising from their atomic size misfit (Figure S1(a) of the [supplementary material](#)) with the displacement of each solvent atom being dependent on the magnitude of the atomic size misfit and the distance from the solute atom. Consequently, the atomic displacement averaged over the entire crystal is expected to increase with increasing solute concentration, although the increase may not occur in a simple way, in particular when the solute concentration is high. It is worthwhile, therefore, to investigate the relationship between the average atomic displacement and the strength of solid solution alloys. Here it is important to note that *all atoms in a HEA are expected to be displaced from the ideal lattice positions*, since multiple principal elements with different sizes interact with each other (Fig. 1(a) and Figure S1(b) of the [supplementary material](#)) unlike in dilute alloys where only those in the close vicinity of the solute atoms are expected to be displaced (Figure S1(a) of the [supplementary material](#)).

In the present study, we investigate the magnitude of the average atomic displacement in the quinary equiatomic HEA CrMnFeCoNi using single-crystal synchrotron X-ray diffraction and first-principles calculations, in order to determine whether it can be used as an alternative scaling factor to predict SSS. We test its applicability to not just the quinary equiatomic HEA, CrMnFeCoNi, but also several of its derivative quaternary and ternary equiatomic alloys: FeCoNi, MnFeCoNi, MnCoNi, MnFeNi, CrCoNi, CrFeCoNi, and CrMnCoNi.

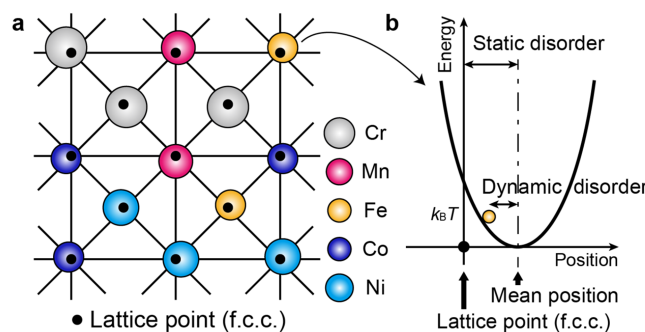


FIG. 1. Static disorder in the CrMnFeCoNi HEA. (a) Schematic illustration of the FCC lattice of the CrMnFeCoNi HEA. The mean positions of the atoms are displaced from the ideal lattice points (the displacements are exaggerated as an aid to the eye). (b) Schematic illustration of an energy-position curve for a harmonic oscillator in thermal equilibrium. The displacement between the mean position and the lattice point is considered as the static disorder whereas the thermal vibration around the mean position is the dynamic disorder.

The magnitude of the atomic displacement parameter (ADP) obtained by X-ray diffraction at finite temperatures is a sum of the squares of the dynamic displacements of all constituent atoms from their mean (equilibrium) positions due to thermal vibration (dynamic disorder) and the static displacement of the mean positions from the ideal lattice points (static disorder) (Fig. 1(b)).²⁸ Therefore, the ADP becomes increasingly dominated by the static component as the temperature is decreased down to cryogenic temperatures. The refined ADP values obtained in the present study at 25 and 300 K are 23.5 ± 0.4 and 58.7 ± 0.5 pm², respectively (details of the single-crystal X-ray diffraction experiment from which these ADP values were obtained are given in Table S1 of the [supplementary material](#)). Based on the ADP value measured at 25 K (23.5 ± 0.4 pm²), the static disorder in the equiatomic CrMnFeCoNi HEA is inferred to be significant, since the static disorder for pure FCC metals is zero (all atoms are perfectly located on the FCC lattice points). The difference (35.2 pm²) between the ADP values at 25 and 300 K is attributed to dynamic disorder (thermal vibration). This value of the dynamic disorder in our equiatomic CrMnFeCoNi HEA with the FCC structure is comparable to that obtained for the equiatomic NbMoTaW alloy with the BCC structure (37 pm²) [Ref. 29]. (The magnitude of dynamic disorder was not measured for the quaternary NbMoTaW alloy but was only estimated from the Debye-Waller factors of the constituent pure elements [Ref. 29].) However, the magnitude of static disorder in our FCC HEA (23.5 pm²) is smaller than that in the BCC-NbMoTaW alloy (55 pm²) [Ref. 30]. (The magnitude of static disorder was not measured for the quaternary NbMoTaW alloy but was estimated from the lattice constants of the constituent pure elements [Ref. 30].) This we believe is due partly to the lower packing efficiency (68%) of the BCC structure compared to that (74%) of the FCC structure (atoms in the BCC structure thus have more space to be displaced) and partly to the much larger atomic radii of the constituent elements in the NbMoTaW alloy (Goldschmidt radii: 140.0 – 146.7 pm) compared to the CrMnFeCoNi HEA (124.0 – 125.3 pm, see Table I).³¹

Having determined the *average* ADP, we were not able to take the next step and determine the *independent* ADPs for each of the constituent elements of the HEA by single-crystal X-ray diffraction, even using anomalous scattering. Therefore, we performed first-principles total-energy calculations to obtain independent mean-square atomic displacements (MSADs) for each of the constituent elements through structural relaxation of a special quasirandom structure (SQS)³² for the

TABLE I. Goldschmidt radii and effective atomic radii of the elements in our HEA. The effective atomic radii are derived by structural relaxation of SQSs for five different quaternary equiatomic alloys.

	Cr	Mn	Fe	Co	Ni
Goldschmidt radius (pm)	124.9	124.0	124.1	125.3	124.6
Effective atomic radius, $r_i^{\text{effective}}$ (pm)	126.9	123.5	121.9	121.9	123.9

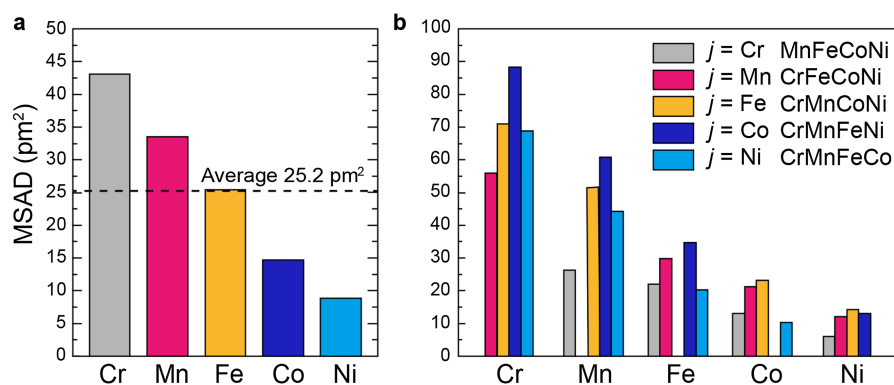


FIG. 2. MSADs of each of the constituent elements. (a) Quinary CrMnFeCoNi HEA, and (b) five different quaternary equiatomic alloys derived by first-principles total-energy calculations for SQSs with the $5 \times 4 \times 4$ and $4 \times 4 \times 4$ FCC supercells, respectively.

quinary HEA. Details are described in the [supplementary material](#).^{32–34} The MSADs for each of the elements are illustrated in Fig. 2(a) together with the average value. The MSAD value monotonically decreases as the atomic number increases. The ADP value experimentally obtained at 25 K for the quinary HEA (23.5 pm^2) agrees fairly well with the theoretically calculated MSAD value averaged over the five elements (25.2 pm^2). To put this in perspective, the difference in the square root of MSAD and ADP ($\sqrt{25.2} - \sqrt{23.5}$) is 0.17 pm , which is much smaller than the difference between the effective atomic radii of Co and Ni (2.0 pm). The individual MSAD values show no correlation with the Goldschmidt radii, which are derived from the atomic bond distance for the corresponding element with coordination number 12 in a wide variety of compounds containing the relevant element³¹ (see Figure S2(a) of the [supplementary material](#)), indicating that the actual atomic radius of each of the constituent elements in the HEA is quite different from the Goldschmidt radius.

In order to estimate the atomic radius for each of the constituent elements in the quinary HEA, the relaxed supercell volumes were calculated for five hypothetical quaternary alloys with different combinations of four of the five elements (MnFeCoNi, CrFeCoNi, CrMnCoNi, CrMnFeNi and CrMnFeCo). The relaxed supercell volumes of these quaternary alloys are quite different from one another (Table II and Figure S3(a) of the [supplementary material](#)), indicating the significantly different atomic volumes of the constituent elements. The quaternary alloy without Co possesses the largest relaxed supercell volume while that without Cr possesses the smallest one. The effective atomic radii of the five elements, $r_i^{\text{effective}}$ ($i = \text{Cr, Mn, Fe, Co, Ni}$), in the quinary HEA can be deduced from the relaxed supercell volumes of the simulated quaternary alloys, as follows. First, an average atomic radius of the four constituent elements in each of the quaternary alloys, $r_{i \neq j}^{\text{average}}$ (j is an element that is not present in the quaternary alloy) is calculated using the following equation,

$$r_{i \neq j}^{\text{average}} = \sqrt[3]{V_{i \neq j} / 4\sqrt{2}N}, \quad (1)$$

where N is the number of atoms in the supercell (256) and $V_{i \neq j}$ is the relaxed supercell volume (see Table II). Then, the effective atomic radii, $r_i^{\text{effective}}$, are calculated by minimizing the

TABLE II. Relaxed supercell volumes of SQSs for the five different quaternary equiatomic alloys.

j	Cr	Mn	Fe	Co	Ni
$i \neq j$	MnFeCoNi	CrFeCoNi	CrMnCoNi	CrMnFeNi	CrMnFeCo
Supercell volume, $V_{i \neq j} (\text{nm}^3)$	2.6811	2.7365	2.7626	2.7633	2.7287

following residual:

$$\delta = \sum_j \left(\prod_{i \neq j} r_i^{\text{effective}} - (r_{i \neq j}^{\text{average}})^4 \right) \quad (j = \text{Cr, Mn, Fe, Co, Ni}). \quad (2)$$

The effective atomic radius decreases in the order Cr, Ni, Mn, Fe and Co, though it must be noted that Fe and Co have virtually the same radii (see Table I and Figure S3(b) of the [supplementary material](#)). This ordering of the effective atomic radii is different from that of the Goldschmidt radii (Table I). Interestingly, the largest pair-wise difference in atomic radii of the five elements (Cr, Mn, Fe, Co, Ni) is much larger for the effective atomic radii (4.1% between Cr and Co) than for the Goldschmidt radii (1.0% between Mn and Co). However, the MSAD values show no correlation with the effective atomic radius (correlation coefficient $R^2 = 0.375$) (see Figure S2(b) of the [supplementary material](#)).

Fig. 2(b) and Table S3 of the [supplementary material](#) clearly indicate that the MSAD of the five elements varies significantly depending on the combination of elements present in the quaternary alloys. For example, the MSAD value (60.9 pm²) for Mn in the CrMnFeNi alloy is more than twice that (26.3 pm²) in the MnFeCoNi alloy. This implies that atomic displacement of a particular element in these equiatomic alloys depends on the combination of constituent atoms present and not just on the radius of an individual atom. In other words, the lattice distortion depends not just on the size of a given atom, but also the environment that it finds itself in (i.e., which other elements are present in the alloy).

The extent of further displacement of the four constituent atoms of the quaternary alloy upon the addition of the fifth element to form the quinary HEA can be estimated from the difference (ΔU_j) between the MSAD value averaged over the four elements ($i \neq j$) in the quinary HEA (U_i^{quinary}) and that in the corresponding quaternary alloy ($i \neq j$) ($U_i^{\text{quaternary}}$), as given by the following equation (see Table S4 of the [supplementary material](#)),

$$\Delta U_j = \frac{1}{4} \left(\sum_{i \neq j} U_i^{\text{quinary}} - \sum_{i \neq j} U_i^{\text{quaternary}} \right) \quad (j = \text{Cr, Mn, Fe, Co, Ni}). \quad (3)$$

The value of ΔU_j tends to increase with increase in the effective atomic radius $r_i^{\text{effective}}$, as shown in Fig. 3. This indicates that atoms with relatively large effective atomic radii tend to displace other smaller atoms significantly. This is the case for Cr with the largest effective atomic radius and the largest (positive) value of ΔU_j . Other elements with smaller effective atomic radii having negative values of ΔU_j tend to be distributed among the larger atoms to better accommodate the displacements. In this sense, Cr plays a crucial role in determining the atomic arrangement, in particular the

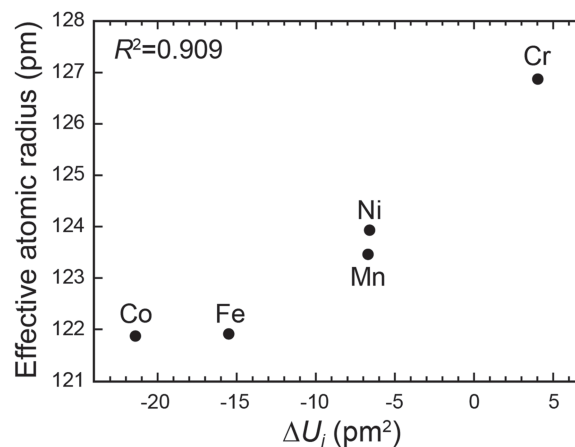


FIG. 3. Effective atomic radii of Cr, Mn, Fe, Co and Ni atoms plotted against ΔU_j , which is the difference between the MSADs averaged over four elements in the quinary HEA and the quaternary alloys. The value of ΔU_j tends to increase with increase in the effective atomic radius $r_i^{\text{effective}}$.

static displacement of the constituent atoms from the ideal FCC positions in the equiatomic quinary HEA.

We now evaluate how well the MSADs, estimated as above, correlate with the strengths of a family of complex, equiatomic, FCC alloys. For this we utilize the results of Wu *et al.*³⁵ who recently investigated the temperature dependence of the yield strength of polycrystals of the quinary CrMnFeCoNi HEA and some of its derivative FCC quaternary and ternary equiatomic alloys with similar grain sizes so that the grain boundary effect can be ignored to first order. The values of yield strength extrapolated to 0 K by fitting their temperature dependences with an exponential function³⁵ are tabulated in Table S5 of the [supplementary material](#). It is of interest to evaluate how the yield strengths of these alloys at 0 K correlate with their MSAD values averaged over the constituent elements. For this purpose, first-principles total-energy calculations were made to deduce MSAD values for four different ternary equiatomic alloys (CrCoNi, MnFeNi, MnCoNi and FeCoNi). As seen in Fig. 4, when normalized by shear modulus,^{36,37} the yield strengths at 0 K deduced by Wu *et al.*³⁵ for these equiatomic ternary, quaternary and quinary alloys scale linearly with the square root of the average MSAD values and can be described by the following equation:

$$\sigma_{YS}/\mu = k \cdot \text{MSAD}^{1/2} (k : \text{constant}) \quad (4)$$

This clearly indicates that the MSAD value can be a good scaling factor in predicting the athermal stress (yield strength at 0 K) of solid solution alloys, especially compositionally complex systems. The square-root scaling in Equation (4) indicates that the resistance exerted by randomly distributed solute atoms to the motion of dislocations in solid solution alloys is determined by the extent to which the crystal is distorted, that is, the degree to which the constituent atoms are displaced from the regular lattice positions. If this is true, we can predict trends in the strengths of other compositionally complex alloys by determining the appropriate MSAD values, as was shown here for the equiatomic quinary HEA, CrMnFeCoNi, and its medium-entropy derivatives. Thus, it may be possible to predict, for example, how the alloy composition should be modified away from the equiatomic composition to achieve the highest strength.

Mechanistically, what is possibly occurring in the HEA during deformation might be similar to that assumed in the SSS model of Labusch,^{4,38} in which dislocations move through random spatial fluctuations in solute density to experience a range of interaction forces from clusters of solutes (weak pinning). To avoid the difficulties in estimating the dislocation-solute interaction forces, here we present a way to quantify the effects of solutes in complex solid solution alloys by taking into account their capability to distort the crystal.

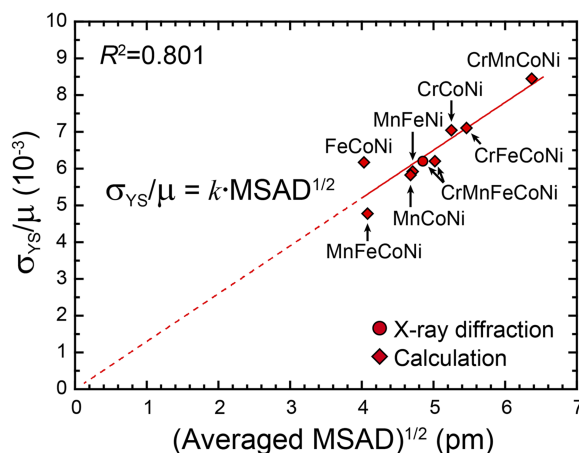


FIG. 4. Yield strengths of the quinary CrMnFeCoNi HEA and its derivative quaternary and ternary equiatomic alloys extrapolated to 0 K [Ref. 35] and normalized by shear modulus^{36,37} plotted against the square root of the MSAD value averaged over the constituent elements.

Moreover, we predict that Equation (4) will be valid also for binary FCC alloys regardless of whether they are in the regime of weak or strong pinning. This is a natural consequence of the hypothesis that the resistance exerted by randomly distributed solute atoms to the motion of dislocations is determined by the extent to which the crystal lattice *on average* is distorted. Although there is debate about the concentration dependence of strength in FCC solid-solution alloys (as exemplified by the $c^{1/2}$ scaling for strong pinning (Fleischer model³) versus the $c^{2/3}$ scaling for weak pinning (Labusch model⁴)), our present results suggest that the scaling of the strength of binary FCC alloys should be made using the MSAD value. In that case, the solute concentration dependence may not have a single value for the power exponent because its influence appears indirectly through the MSAD. If true, the MSAD value is the universal scaling factor to predict the strength of solid solutions of crystals having a small frictional stress (of the Peierls-type) for dislocation motion. To test our prediction, the applicability of Equation (4) to binary FCC solid solution alloys over a wide range of solute concentration is currently under investigation.

In summary, the atomic displacement parameter in the equiatomic CrMnFeCoNi HEA with the FCC structure has been measured by single-crystal synchrotron X-ray diffraction and the static component of the atomic displacement is found to be significant (23.5 pm^2). The independent MSADs of each of the constituent elements in the HEA deduced by first-principles total-energy calculations for an SQS representing the disordered structure of the HEA monotonically decreases with increasing atomic number. They correlate neither with the Goldschmidt radii nor with the effective atomic radii derived from the structural relaxation of five different SQSs of quaternary alloys consisting of combinations of four of the five elements. The MSADs of the five elements considered here (Cr, Mn, Fe, Co, Ni) vary significantly depending on the combination of elements present in the alloys and cannot be determined solely by their atomic radii. That is, the average lattice distortion due to any given element depends not just on its own effective radius but which other elements are present in the alloy. The modulus-normalized strength at 0 K of eight FCC solid solution alloys, the quinary equiatomic CrMnFeCoNi HEA and its derivative quaternary and ternary equiatomic alloys, is found to be proportional to the square root of the relevant MSAD values, indicating that the MSAD value is a valuable scaling factor for predicting the athermal stress (yield strength at 0 K) of solid solution alloys. This is significant because it implies that the resistance to dislocation motion exerted by randomly distributed solute atoms is determined solely by the extent to which the crystal is distorted and we can therefore predict the trends in the strength of other FCC solid solution alloys by determining the appropriate MSAD values.

SUPPLEMENTARY MATERIAL

See [supplementary material](#) for details of sample preparation, synchrotron X-ray diffraction and first-principles calculations. Figures S1-S3 and Tables S1-S5 of the [supplementary material](#) are also provided.

ACKNOWLEDGMENTS

The study was conceived during a short-term research stay by E.P.G. in the group of H.I. at Kyoto University sponsored by an invitation fellowship of JSPS; the HEA was fabricated while E.P.G. was at the Oak Ridge National Laboratory funded by the U.S. Department of Energy, Office of Science, Basic Energy Sciences, Materials Sciences and Engineering Division. E.P.G. acknowledges DFG funding in Germany through project GE 2736/1-1. This work was also supported by JSPS KAKENHI grant numbers 15H02300, 16K14373 and 16K14415, and the Elements Strategy Initiative for Structural Materials (ESISM) from the Ministry of Education, Culture, Sports, Science and Technology (MEXT) of Japan, and in part by Advanced Low Carbon Technology Research and Development Program (ALCA) from the Japan Science and Technology Agency (JST). The synchrotron radiation experiments were performed at the BL02B1 of SPring-8 with the approval of the Japan Synchrotron Radiation Research Institute (JASRI) (Proposal Nos. 2014B1228, 2014B1553, 2015A1468 & 2016B1096). We wish to thank Dr K. Sugimoto and Dr N. Yasuda for their assistance at the BL02B1 of SPring-8.

- ¹ N. F. Mott and F. R. N. Nabarro, Report of the Conference on Strength of Solids **1** (1948).
- ² F. R. N. Nabarro, *Proc. Phys. Soc.* **58**, 669 (1946).
- ³ R. L. Fleishcer, in *The Strengthening of Metals*, edited by D. Peckner (Reinhold Pub. Co. Ltd., New York, 1964).
- ⁴ R. Labusch, *Phys. Status Solidi* **41**, 659 (1970).
- ⁵ G. P. M. Leyson, W. A. Curtin, L. G. Hector, and C. F. Woodward, *Nat. Mater.* **9**, 750 (2010).
- ⁶ G. P. M. Leyson, L. G. Hector, and W. A. Curtin, *Acta Mater.* **60**, 3873 (2012).
- ⁷ G. P. M. Leyson, L. G. Hector, and W. A. Curtin, *Acta Mater.* **60**, 5197 (2012).
- ⁸ C. Varvenne, A. Luque, and W. A. Curtin, *Acta Mater.* **118**, 164 (2016).
- ⁹ I. Toda-Caraballo, E. I. Galindo-Nava, and P. E. J. Rivera-Diaz-del-Castillo, *Acta Mater.* **75**, 287 (2014).
- ¹⁰ I. Toda-Caraballo and P. E. J. Rivera-Diaz-del-Castillo, *Acta Mater.* **85**, 14 (2015).
- ¹¹ I. Toda-Caraballo, J. S. Wrobel, S. L. Dudarev, D. Nguyen-Manh, and P. E. J. Rivera-Diaz-del-Castillo, *Acta Mater.* **97**, 156 (2015).
- ¹² I. Toda-Caraballo and P. E. J. Rivera-Diaz-del-Castillo, *Intermetallics* **71**, 76 (2016).
- ¹³ I. Toda-Caraballo, *Scripta Mater.* **127**, 113 (2017).
- ¹⁴ D. C. Ma, M. Friak, J. von Pezold, D. Raabe, and J. Neugebauer, *Acta Mater.* **85**, 53 (2015).
- ¹⁵ D. Ma, M. Friak, J. von Pezold, J. Neugebauer, and D. Raabe, *Acta Mater.* **98**, 367 (2015).
- ¹⁶ J. W. Yeh, S. K. Chen, S. J. Lin, J. Y. Gan, T. S. Chin, T. T. Shun, C. H. Tsau, and S. Y. Chang, *Adv. Eng. Mater.* **6**, 299 (2004).
- ¹⁷ B. Gludovatz, A. Hohenwarter, D. Catoor, E. H. Chang, E. P. George, and R. O. Ritchie, *Science* **345**, 1153 (2014).
- ¹⁸ Z. Li, K. G. Pradeep, Y. Deng, D. Raabe, and C. C. Tasan, *Nature* **534**, 227 (2016).
- ¹⁹ E. J. Pickering and N. G. Jones, *Int. Mater. Rev.* **61**, 183 (2016).
- ²⁰ X. Z. Lim, *Nature* **533**, 306 (2016).
- ²¹ Z. J. Zhang, M. M. Mao, J. W. Wang, B. Gludovatz, Z. Zhang, S. X. Mao, E. P. George, Q. Yu, and R. O. Ritchie, *Nat. Commun.* **6** (2015).
- ²² T. M. Smith, M. S. Hooshmand, B. D. Esser, F. Otto, D. W. McComb, E. P. George, M. Ghazisaeidi, and M. J. Mills, *Acta Mater.* **110**, 352 (2016).
- ²³ B. Cantor, I. T. H. Chang, P. Knight, and A. J. B. Vincent, *Mater. Sci. Eng., A* **375**, 213 (2004).
- ²⁴ A. Gali and E. P. George, *Intermetallics* **39**, 74 (2013).
- ²⁵ F. Otto, A. Dlouhy, C. Somsen, H. Bei, G. Eggeler, and E. P. George, *Acta Mater.* **61**, 5743 (2013).
- ²⁶ P. Haasen, in *Dislocations in Metallurgy*, edited by F. R. N. Nabarro (North-Holland, Amsterdam, Netherlands, 1979), Vol. 4, pp. 155.
- ²⁷ P. Haasen, in *Physical Metallurgy*, edited by R. W. Cahn and P. Haasen (Elsevier Science, 1996), Vol. 3, pp. 2009.
- ²⁸ J. D. Dunitz, V. Schomaker, and K. N. Trueblood, *J. Phys. Chem.* **92**, 856 (1988).
- ²⁹ Y. Zou, S. Maiti, W. Steurer, and R. Spolenak, *Acta Mater.* **65**, 85 (2014).
- ³⁰ J. W. Yeh, S. Y. Chang, Y. D. Hong, S. K. Chen, and S. J. Lin, *Mater. Chem. Phys.* **103**, 41 (2007).
- ³¹ V. M. Goldschmidt, *Z. Phys. Chem.* **133**, 397 (1928).
- ³² A. Zunger, S. H. Wei, L. G. Ferreira, and J. E. Bernard, *Phys. Rev. Lett.* **65**, 353 (1990).
- ³³ K. Yuge, *J. Phys. Soc. Jpn.* **84**, 084801 (2015).
- ³⁴ G. Kresse and J. Furthmüller, *Phys. Rev. B* **54**, 11169 (1996).
- ³⁵ Z. Wu, H. Bei, G. M. Pharr, and E. P. George, *Acta Mater.* **81**, 428 (2014).
- ³⁶ G. Laplanche, A. Kostka, O. M. Horst, G. Eggeler, and E. P. George, *Acta Mater.* **118**, 152 (2016).
- ³⁷ A. Haglund, M. Koehler, H. Bei, V. Keppens, and E. P. George, to be published.
- ³⁸ R. Labusch, *Acta Metall.* **20**, 917 (1972).